Polarizer-free liquid crystal display with double microlens array layers and polarization-controlling liquid crystal layer

You-Jin Lee,[1,3] Chang-Jae Yu,[1,2,3] and Jae-Hoon Kim[1,2,*]

[1]*Department of Electronic Engineering, Hanyang University, Seoul 133-791, South Korea*
[2]*Department of Information Display Engineering, Hanyang University, Seoul 133-791, South Korea*
[3]*These authors contributed equally to this work.*
[*]*jhoon@hanyang.ac.kr*

Abstract: We propose a polarizer-free liquid crystal display (LCD) consisting of two microlens array (MLA) layers, a twisted nematic (TN) LC layer, and two light-blocking masks. By changing the polarization state, focal length of the LCD can be controlled. Since two light-blocking masks have a circular stop pattern and a complementary open pattern, entire gray-scale spectrum may be realized by controlling the intensity of light passing through masks. Ultimately, fast response time characteristics could be achieved due to the alignment of LC molecules on the flat MLA surface.

OCIS codes: (120.2040) Displays; (230.3720) Liquid-crystal devices.

References and links

1. J. W. Doane, N. A. Vaz, B.-G. Wu, and S. Zumer, "Field controlled light scattering from nematic microdroplets," Appl. Phys. Lett. **48**(4), 269–271 (1986).
2. I. Shiyanovskaya, S. Green, A. Khan, G. Magyar, O. Pishnyak, and J. W. Doane, "Substrate-free cholesteric liquid crystal display," J. Soc. Inf. Disp. **16**(1), 113–115 (2008).
3. G. H. Heilmeier and L. A. Zanoni, "Guest-host interactions in nematic liquid crystals. A new electro-optic effect," Appl. Phys. Lett. **13**(3), 91–93 (1968).
4. D. L. White and G. N. Taylor, "New absorptive mode reflective liquid crystal display device," J. Appl. Phys. **45**(11), 4718–4723 (1974).
5. Y.-H. Lin, H. Ren, S. Gauza, Y.-H. Wu, X. Liang, and S.-T. Wu, "Reflective direct-view displays using a dyedoped dual-frequency liquid crystal gel," J. Disp. Technol. **1**(2), 230–233 (2005).
6. Y. W. Kim, J. Jeong, S. H. Lee, J.-H. Kim, and C.-J. Yu, "Single polarizer liquid crystal display mode with fast response," Mol. Cryst. Liq. Cryst. **543**(1), 101–106 (2011).
7. Y.-J. Lee, J.-H. Baek, Y. Kim, J. U. Heo, Y.-K. Moon, J. S. Gwag, C.-J. Yu, and J.-H. Kim, "Polarizer-free liquid crystal display with electrically switchable microlens array," Opt. Express **21**(1), 129–134 (2013).
8. G. Zhao and P. Mouroulis, "Diffusion model of hologram formation in dry photopolymer materials," J. Mod. Opt. **41**(10), 1929–1939 (1994).
9. S. Piazzolla and B. K. Jenkins, "Dynamics during holographic exposure in photopolymers for single and multiplexed gratings," J. Mod. Opt. **46**(15), 2079–2110 (1999).
10. Y. W. Kim, J. Jeong, S. H. Lee, J.-H. Kim, and C.-J. Yu, "Improvement in switching speed of nematic liquid crystal microlens array with polarization independence," Appl. Phys. Express **3**(9), 094102 (2010).
11. Y.-J. Lee, Y.-K. Kim, S. I. Jo, J. S. Gwag, C.-J. Yu, and J.-H. Kim, "Surface-controlled patterned vertical alignment mode with reactive mesogen," Opt. Express **17**(12), 10298–10303 (2009).
12. Y.-J. Lee, C.-J. Yu, Y.-K. Kim, S. I. Jo, and J.-H. Kim, "Direct image of a molecular orientation of liquid crystal using directional polymerization of photoreactive mesogen," Appl. Phys. Lett. **98**(3), 033106 (2011).

1. Introduction

Liquid crystal displays (LCD) have been widely utilized in flat panel displays and various optical applications due to their high performance characteristics and low power consumption. Because LCDs use the anisotropic optical properties of LCs to control the properties of the incident light, optical components such as polarizers and optical compensators must be included in the devices. Unfortunately, these optical elements limit the transmittance characteristics and increase the device cost. In LCDs, a polarizer situated in

#249093 Received 1 Sep 2015; revised 6 Oct 2015; accepted 7 Oct 2015; published 12 Oct 2015

front of the backlight unit can reduce the amount of available light by 50%. To eliminate the need for polarizers in LCDs, polymer-dispersed LC, cholesteric LC, and guest-host LC modes have been suggested [1–5]. However, specific problems such as a low contrast ratio, high driving voltage, and slow response time characteristics are associated with these modes.

In our previous work, we described an LCD mode with a single polarizer based on a microlens array (MLA) [6]. While a low driving voltage and fast response time characteristics could be achieved with the devised system, the transmittance was still low and the display showed polarization-dependent properties. In a subsequent report, we detailed a polarizer-free LCD that uses an electrically switchable LC MLA with light-blocking layers [7]. This device allowed the entire grayscale spectrum to be realized with a high contrast ratio by controlling the electric field. However, the response time characteristics were still slow because the LC molecules possessed a spiral structure on the indented lens surface.

In this paper, we propose a polarizer-free LCD containing two MLA layers and an LC layer with light-blocking masks. The twisted nematic LC mode changes the polarization state and refractive index of incident light based on the applied voltage. As a result of index matching between the polymer lens and the LC layer, the MLA can change the focal length. In addition, by adopting both a circular stop mask and a complementary open mask, grayscales as well as black and dark device states can be realized depending on the focusing state of the MLA with the LC layer.

2. Operating principle

Figure 1 shows the operating principle of the proposed polarizer-free LCD. The pixels consisted of switching, focusing, and light-blocking components. Here, a twisted nematic LC mode sandwiched between two focusing parts was employed as the switching element. The focusing part was composed of a surface relief structure filled with a liquid crystalline polymer (LCP). Due to the birefringence property of the LCP, the focusing assembly exhibited polarization-dependent characteristics. The light-blocking parts consisted of a circular light stop mask (the first black matrix (BM)) and a complementary open mask (the second BM).

In the absence of an applied voltage, the LC layer changes the polarization direction of light due to waveguide effect of the twisted nematic LC mode. The incident *x*-axis beam passes through the top MLA layer without any change because the refractive index of the surface relief polymer is identical to the ordinary refractive index of the LCP. The polarization direction of the *x*-axis light is then changed to the *y*-axis after passing through the LC layer. The *y*-axis polarized light goes through second MLA layer without any change due to same reason given above for the first MLA layer. This light is then blocked at second BM layer. The incident *y*-axis beam is subsequently refracted at the interface between the lens polymer and LCP layers as a result of the different refractive indices of the materials. However, the direction of polarization is maintained. Upon passing through the LC layer, the direction of the light is changed to the *x*-axis. The light is then refracted and focused due to the difference between the refractive index of the polymer and the extraordinary refractive index of the LCP. Ultimately, the light is blocked at the first BM layer, resulting in a black state when no voltage is applied.

When an electric field is applied to the cell, the LC molecules are raised and aligned vertically with a positive dielectric constant, and the effective refractive index is equivalent to the ordinary refractive index of the LC. The incident *x*-axis beam passes through the top MLA and LC layers without any change, but is refracted at the interface between the polymer and LCP layers. The light then passes the light blocking layers because its focal length is longer than the distance of the f_2-plane. The incident *y*-axis beam is refracted at the interface between the lens polymer and LCP layers. The polarization direction of the light is maintained after the LC layer, and the beam passes through the second MLA layer without refraction. As this

#249093 Received 1 Sep 2015; revised 6 Oct 2015; accepted 7 Oct 2015; published 12 Oct 2015

light also passes the two blocking layers, the cell shows a white state under an applied voltage.

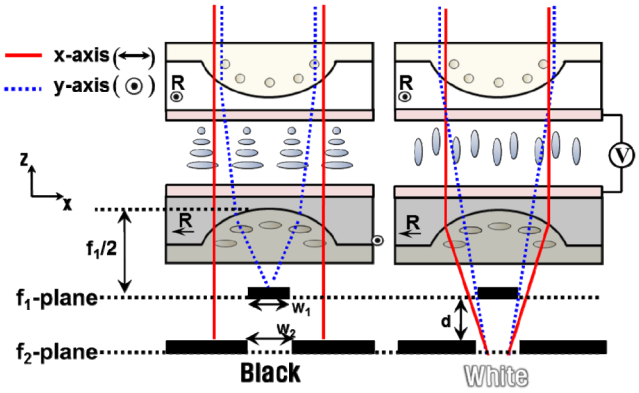

Fig. 1. Schematic diagram of the proposed polarizer-free LCD.

3. Experiments

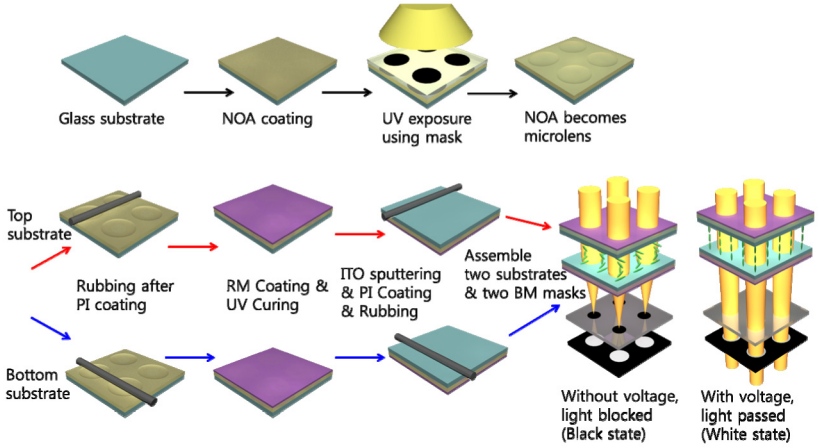

Fig. 2. Schematic diagram of the LCD fabrication process.

A schematic diagram of the LCD fabrication process is shown in Fig. 2. The BM layers were patterned on both sides of a cleaned glass substrate with aluminum (Al) using a conventional lift-off photolithographic method. The diameter and pitch of the circular stop mask (the first BM) were 50 μm and 200 μm, respectively. The circle size was selected by considering the focused beam size at the voltage off state. For the complementary open mask (the second BM), the diameter and pitch were 40 μm and 200 μm, respectively. The size of the open circles was designed smaller than the circle size of the 1st BM for good black property. To prepare the MLA layer, a UV-curable polymer (NOA60, Norland, n_p = 1.56) was first spin-coated onto a glass substrate. The polymer was then exposed to UV light passed through a photomask (100 μm diameter, 200 μm pitch) for 60 s. The spatial modulation of the UV light intensity produced a variation in the monomer density and thus, UV-curable monomers diffused from blocked regions to unblocked areas so as to maintain the relative monomer density [8,9]. For complete polymerization of the surface relief structure, irradiation with UV light was performed for 10 min without a photomask. Next, a planar alignment material (RN1199, Nissan Chemical) was spin-coated onto the surface relief structure and rubbed unidirectionally. The rubbing directions for the top and bottom MLA layers were along the *y*-

#249093 Received 1 Sep 2015; revised 6 Oct 2015; accepted 7 Oct 2015; published 12 Oct 2015

axis and *x*-axis, respectively. Finally, LCP (RMS03-001C, Merck) was spin-coated onto the surface relief structure twice and irradiated with UV light for 10 min to ensure polymerization. The extraordinary (n_e) and ordinary (n_o) refractive indices were 1.68 and 1.54, respectively. A sputtered indium tin oxide (ITO) layer was utilized as an electrode, and RN1199 was coated and rubbed cross-wise on both the top and bottom substrates in a direction identical to the alignment of the LCP. To maintain the cell thickness, 3.0 μm glass spacers were employed. The nematic LC (ZKC5085, Chisso, n_e = 1.650, n_o = 1.499) was injected into the cell by the capillary effect at room temperature.

4. Results and discussion

Figure 3(a) shows a cross-sectional scanning electron microscopy (SEM) image of the fabricated MLA. The UV-curable polymer formed the lens structure while the LCP layer appeared to be flat and uniform. Figure 3(b) displays the microscopic texture under crossed polarizers and the optical axis of the LCP according to a polarizer. The black state indicated that the LCP was well aligned unidirectionally. In Fig. 3(c), the cell rotated by 45° with respect to the polarizers exhibits both the white state and focusing properties. The measured pitch (p) and depth (t) of the lens were 200 μm and 11 μm, respectively. Using the spherical model, the radius of curvature (R) of the lens was calculated to be about 350 μm, and the resultant focal length determined the position of the two BM masks.

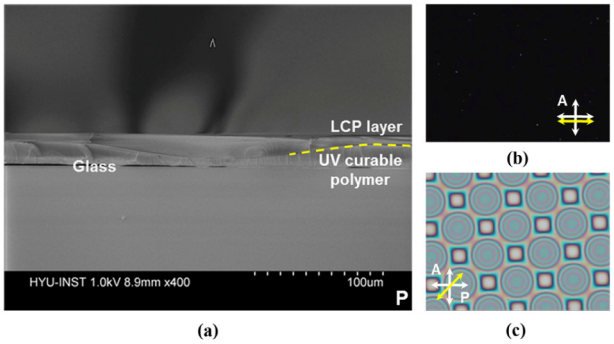

Fig. 3. (a) Cross-sectional SEM image of the MLA and microscopic textures under crossed polarizers (b) in same rubbing direction and (c) rotated by 45° with respect to the polarizer.

Figure 4 shows the optical system for calculating the position of the BM layers. The distance between the two lenses (*d*) and the depth of the lens (*t*) were on the order of micrometers, while the focal length was on the order of millimeters. Therefore, d and t were neglected and the focal lengths of the two lenses (f_1 and f_2) were approximately the same. The focal length of light through two lenses could be calculated according to expression.

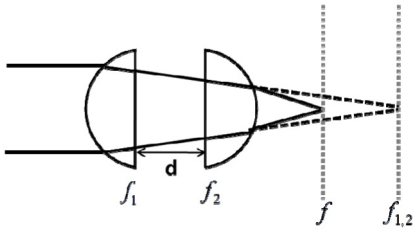

Fig. 4. Schematic diagram of the optical system.

The calculated f and f_1 (or f_2) were 1.4 mm and 2.9 mm, respectively. These values were in good agreement with the measured f and f_1 (or f_2) of 1.1 mm and 2.3 mm, respectively; the discrepancies in the lengths can be attributed to the difference in the refractive indices n_p and

#249093 Received 1 Sep 2015; revised 6 Oct 2015; accepted 7 Oct 2015; published 12 Oct 2015

no. Based on these results, the blocking and complementary open masks were positioned at 1.1 mm and 2.3 mm, respectively.

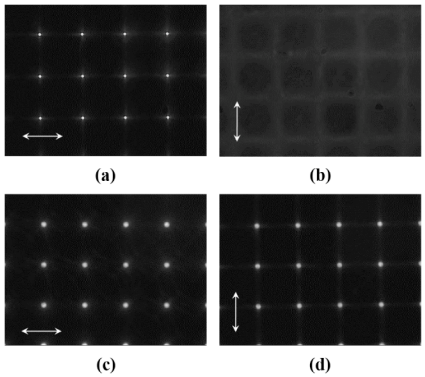

Fig. 5. Microscopic textures at the first BM layer position for (a) x-axis and (b) y-axis polarized light without applied voltage, and (c) x-axis and (d) y-axis polarized light with an applied voltage.

Figure 5 displays the microscopic textures at the *f* position (the first BM position, 1.1 mm) depending on the polarization direction of incident light with and without an applied voltage. In the absence of an electric field, the *x*-axis polarized light (Fig. 5(a)) was focused. This light was refracted twice and will be blocked at the first BM mask. In contrast, the *y*-axis polarized light was defocused (Fig. 5(b)) and will be blocked at the first and second BM masks. Under an electric field, a wider light beam is observed because the incident light, which is refracted once, has a longer focal length (f_1) in the *x*-, and *y*-axis directions (Figs. 5(c) and 5(d)). Consequently, the light could pass through the two BM masks. The focusing properties could be confirmed by measuring the spatial light intensity profile at the focal plane (*f*). For verifying the focusing properties, we checked spatial profile of light intensity at the 1st focal plane with unpolarized light. At the center of the microlens, the beam profile resembles a Gaussian function. During the voltage off state, the beam has a higher intensity and presents a narrower curve (Fig. 6(a)). However, at the voltage on state (10 V), the beam has a lower intensity and produces a wider curve when compared to the case of no applied voltage (Fig. 6(b)). The full grayscale spectrum could thus be realized in the cell with two BM masks by controlling the applied voltage.

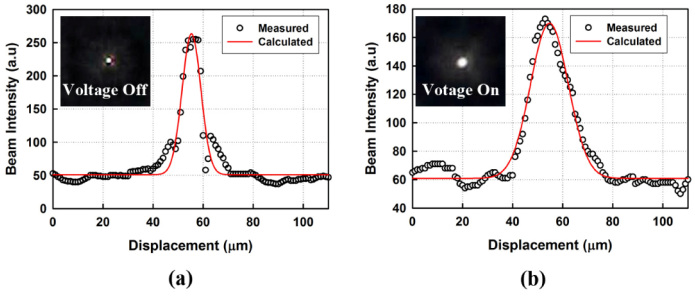

Fig. 6. Beam profiles and textures for (a) voltage off and (b) voltage on states at the 1st focal plane.

Figure 7(a) shows the transmittance characteristics measured with an unpolarized He-Ne laser. The electro-optic switching properties are similar to those of a conventional black TN mode. Furthermore, the light efficiency of the fabricated sample was measured to be 18%. This efficiency value is somewhat low due to the aperture ratio of the two BM layers and the

#249093 Received 1 Sep 2015; revised 6 Oct 2015; accepted 7 Oct 2015; published 12 Oct 2015

MLA. If the circular size of the two BM layers was optimized and a lens arrangement such as hexagonal structure was employed, the light efficiency can be increased. If we adapt a hexagonal structure, the light efficiency will be increase about 20%. And also, if we use the micro-transfer molding method for fabricating the microlens, we can additionally increase the light efficiency because the aberration of the microlens can be decreased. Images showing the microscopic textures at each applied voltage are displayed as insets in Fig. 7(a).

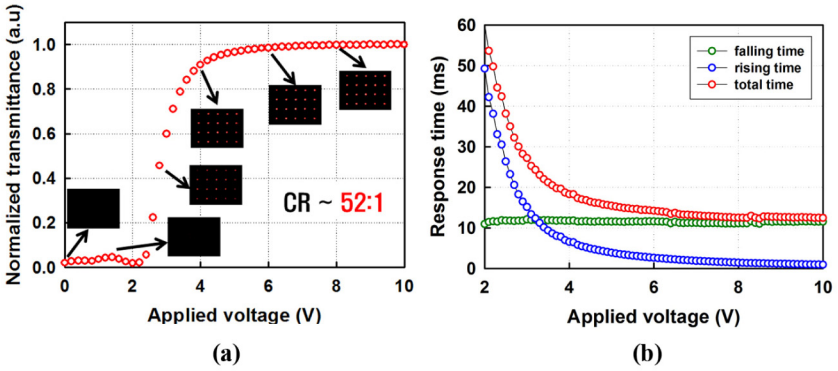

Fig. 7. (a) The obtained voltage-transmittance characteristics; microscopic images corresponding to each applied voltage are displayed as insets, and (b) the voltage-response time characteristics.

The response time characteristics depending on the applied voltage are presented in Fig. 7(b). In our previous work [9], we evaluated the response time properties on the relief structure. The switching speed of the LC molecules was found to be very slow (~1.2 s) because the effective electric field on the LC layer is different at every position and the LC molecules undergo a two-step switching process [10]. While the incorporation of polymerized reactive mesogens within the alignment layer [11, 12] served to improve the response time (85 ms), the obtained value was still rather slow. In the system proposed herein, the response time characteristics improved significantly to 12 ms at 8 V due to both the alignment of LC molecules on a flat surface and the TN structure.

5. Conclusions

In this study, a polarizer-free LCD with two MLA layers, a TN LC layer, and two light blocking masks was utilized to control the polarization state of incident light. In the absence of an applied voltage, *y*-axis light was refracted twice while passing through the MLA layers and blocked at the first BM circles. In contrast, *x*-axis light passed straight through and was ultimately blocked at the second BM layers because the TN LC layer changed the polarization direction of incident light. Under an applied electric field, the incident light was refracted once and had a long focal length. Since this light passed through the two BM layers, a white state was achieved. As a result, the entire grayscale spectrum could be realized by controlling the electric field. Fast response time characteristics were also obtained due to the formation of a flat surface for aligning the LC molecules.

Acknowledgements

This research was supported by the ICT R&D program of MSIP/IITP (10041416, The core technology development of light and space adaptable energy-saving I/O platform for future advertising service) and LG Display Co., Ltd.

#249093 Received 1 Sep 2015; revised 6 Oct 2015; accepted 7 Oct 2015; published 12 Oct 2015